ISSN EN TRÁMITE

AI·E·P
Artificial Intelligence on Electronics and Photonics

Recibido: 15 de enero de 2024
Aceptado: 20 de agosto de 2024
Publicado: 5 de agosto de 2025

Cómo citar:
Bermúdez-Chou, A. C., Morales-Cruzado, B. & Pérez-Gutiérrez, F. G. "Generation of LIPSS in aluminum thin films". *Artificial Intelligence on Electronics and Photonics* **1**(1) pp. 1-8. (2025).

GENERATION OF LIPSS IN ALUMINUM THIN FILMS

Generación de LIPSS en películas delgadas de aluminio

A. C. Bermúdez-Chou[1*], B. Morales-Cruzado[2], F. G. Pérez-Gutiérrez[3]

[1] *Facultad de Ingeniería, Universidad Autónoma de San Luis Potosí, Av. Manuel Nava No. 8, San Luis Potosí, S.L.P. 78290, México.* ORCID: 0000-0003-0581-0283.
[2] *Conahcyt- Centro de Investigaciones en Óptica, A.C., Loma del Bosque 115, Colonia Lomas del Campestre, León, Gto, 37150 México.* ORCID: 0000-0003-1144-657X.
[3] *Facultad de Ingeniería, Universidad Autónoma de San Luis Potosí, Av. Manuel Nava No. 8, San Luis Potosí, S.L.P. 78290, México.* ORCID: 0000-0003-3172-2068.
* Autor de correspondencia: *alienabdezchou@gmail.com*

KEYWORDS:
LIPSS; optical properties; periodicity; structures.

PALABRAS CLAVE:
LIPSS; propiedades ópticas; periodicidad; estructuras.

Abstract

Laser-Induced Periodic Surface Structures (LIPSS) have been reported in the literature for over three decades. These structures can be generated in almost any material. These structures can control the surfaces' optical, chemical, electrical, and mechanical properties. It has been shown that the spatial characteristics of LIPSS depend on the material's optical, thermal, and physical properties (such as roughness r) and irradiation parameters. The main parameters that influence these characteristics are periodicity Λ, height H, and orientation. This work aims to investigate the creation of LIPSS in thin aluminum films. For that, an experimental setup to fabricate these structures was built. The model consists of a six ns pulsed IR (1064 nm) laser with energy up to 20 mJ. Laser scans were created at a speed 8 μm/s (N_{eff} = 4) with f_{rep} = 1 Hz and F_p = 16.2 J/cm^2, with a separation distance Δγ = 60 μm on thin aluminum films. The substrates used to deposit the Al thin films were 8 mm × 40 mm, while the thickness of the thin films was 1 μm. The resulting structure is 300 nm deep.

Resumen

Las estructuras de superficie periódicas inducidas por láser (LIPSS, por sus siglas en inglés) han sido reportadas durante más de tres décadas. Estas estructuras se pueden generar en casi cualquier material y pueden controlar las propiedades ópticas, químicas, eléctricas y mecánicas de las superficies. Se ha demostrado que las características espaciales de LIPSS dependen de las propiedades ópticas, térmicas y físicas del material (como la rugosidad r) y los parámetros de irradiación. Entre los principales factores influenciados en estas características, se encuentran la periodicidad Λ, la altura H y la orientación. En este trabajo se investiga la creación de LIPSS en películas delgadas de aluminio. Para ello se construyó el arreglo experimental con el que se propone fabricar estas estructuras. Se utilizó un láser IR pulsado de 6 ns (1064 nm) con energía de hasta 20 mJ. Los barridos se crearon a una velocidad de 8 μm/s (N_{eff} = 4) con f_{rep} = 1 Hz y F_p = 16.2 J/cm^2, con una distancia de separación Δγ = 60 μm. Las películas delgadas de aluminio tienen unas dimensiones de 8 mm × 40 mm y un espesor de película de 1 μm, estas LIPSS tienen una profundidad aproximada de 300 nm.

1. Introduction

The power and duration of a pulsed laser beam have a crucial influence on the interaction of a laser beam with materials. A certain material absorbs a fraction of light energy, converting it into heat, which is then conducted into the material over long time scales. If the beam is powerful enough, it will melt the material and lead to heat buildup in the surrounding areas. Different parameters can modify these physical processes involving the laser-matter interaction during materials processing [1].

Under certain conditions, exposure of a solid surface to a laser beam gives rise to the formation of Laser-Induced Periodic Surface Structures (LIPSS), which have been reported for over three decades. Some materials where LIPSS have been reported include quartz-copper, aluminum (Al), semiconductors (Ge, Si), and other metals. This is a phenomenon that can be generated in almost any material in a linear consistent way with linearly polarized radiation; these structures can be produced with pulsed laser light, and depending on the material and irradiation parameters, different characteristics are obtained [2-6].

Cavitation erosion is a significant problem in fluid systems such as hydraulic turbines, ship propellers, and water pumps, where the kinetic energy exerted by collapsing vapor bubbles causes surface damage. Due to this inconvenience, many materials linked to different engineering processes have been applied to prevent such phenomena [7]. Although little attention has still been paid to the resistance to cavitation erosion on these surfaces, instead of hardening the material, these structures could dampen the cavitation dynamics [8].

Developing LIPSS manufacturing techniques through micro and nano laser processing on different materials is relevant for medical and technological applications. These LIPSS can potentially improve resistance to cavitation erosion [8], and further research is required to understand its behavior and applications in this field.

This work aims to obtain the parameters for fabricating LIPSS in Al thin films using a nanosecond pulsed laser. The material's optical and surface properties can be altered, this would help mitigate the effects of cavitation.

2. Methods

In this study, the experimental setup shown in Figure 1 was used. It consists of a Q-switched, Nd: YAG, laser emitting 6 ns pulses with maximum energy per pulse of 40 mJ at a 1064 nm wavelength with repetition rate up to 15 Hz (Continuum brand and Minilite model). As shown in Figure 1, the laser beam is directed towards the sample using a series of mirrors, while a couple of irises with a 2 *mm* and 4 mm aperture aim to control the size of the laser spot. An aspheric (f = 8 *mm*) lens focuses the beam on the sample's surface.

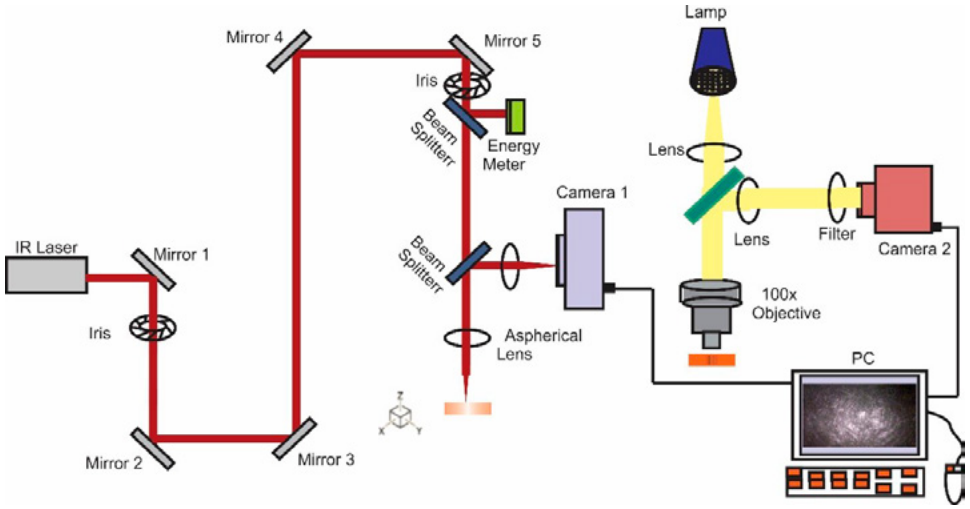

Figure 1.

Implementation of the experimental arrangement for forming the LIPSS.

The sample is then placed on a translation stage that allows movement in the x, y, and z axes. These degrees of freedom will precisely position the sample in the beam path. Sample displacements are controlled through Kinesis software, which provides a velocity range of 0 $\mu m/s$ to 2400 $\mu m/s$.

A 30:70 Reflection-Transmission beam splitter was placed in the laser path to monitor pulse energy in this experimental setup. Light reflected from the beam splitter is directed to an energy meter (JUNO, Ophir). This reading was calibrated to the laser energy incident on the sample.

A separate section of the experimental setup serves to visualize the structure of the samples, which consists of a halogen lamp (QTH10, Thorlabs) as an illumination source, a condenser lens ($f = 100\ mm$) is a 50:50 beam splitter that transmits light to a microscope objective (100x E Plan, Nikon). Light reflected from the sample is transmitted through the microscope objective, which forms an image of the sample brought to a video camera 2 (PL-B776F, Pixelink) with a biconvex lens ($f = 50\ mm$).

Implementing experimental characterization of the laser beam by processing images captured from camera 1 provides a practical and effective alternative for determining the laser spot size and calculating laser fluence. This approach offers several advantages and merits, contributing to the comprehensive understanding and control of the laser beam profile.

A Gaussian function can describe the transverse intensity profile of the laser beam. When the aspheric lens focuses this beam, the wavefront converges at the focal plane, where the beam diameter reaches its minimum value, known as the beam waist, as shown in Figure 2. The radius of the beam at the focal plane is represented by and is defined as the point where the maximum

intensity decays to $\frac{1}{e^2}$. It is possible to obtain the average value of $\omega_{0,}$ from the Gaussian beam propagation theory [9] through expression:

$$2\omega_0 = 4\frac{\lambda f}{\pi D} \tag{1}$$

Where:
λ: Laser wavelength
f: Lens focal length
D: Beam diameter incident on the lens

This expression provides an estimate of the average size of the beam waist in the focal plane, which is useful for evaluating and controlling laser fluence during materials processing.

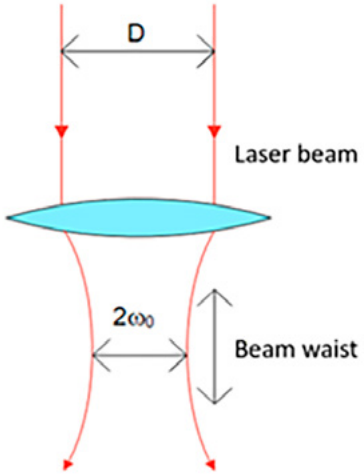

Figure 2.

Propagation of a Gaussian laser beam through a lens.

In this project, LIPSS patterns are generated on Al thin film with a thickness of 1 μm. The generation of these patterns is achieved through the process of laser ablation, which involves the removal of material from a solid sample by converting optical energy into thermal energy through the excitation of electrons. When the fluence of the laser pulse (F_p) exceeds a specific threshold for the material, chemical bonds break, and the material begins to be ejected [1].

Each material has a laser ablation threshold fluence at specific laser pulse duration and wavelength. This threshold per pulse laser fluence is crucial to establish the proper laser ablation conditions and generate LIPSS patterns in the Al thin film. From this value, the fluence parameters and pulse duration can be adjusted to achieve the fluence necessary for controlled ablation and the formation of the desired patterns.

Within the framework of the experiment, a strategy is implemented to generate a matrix of irradiation points on Al thin films. Variations are carried out using two key parameters: the per pulse laser fluence and the number of pulses deposited at each irradiation point.

This experimental approach allows us to explore how different combinations of per-pulse fluence and several pulses influence the formation of LIPSS patterns in Al thin films. The objective is determining the optimal values to generate the most desirable LIPSS patterns. The implemented variations aim to identify the most appropriate experimental conditions to obtain the desired results regarding the formation and characteristics of the LIPSS patterns.

The study of LIPSS has received a lot of attention due to its applications in surface functionalization [9]. It is essential to explore the ability of LIPSS to nanostructure large surface areas.

To generate LIPSS in large areas, laser scans of the sample are necessary. Therefore, the scanning speed (v) must be considered, which is determined by the effective number of pulses deposited (*Neff*). The scan speed can be calculated using Equation 2 [9]:

$$v = \frac{2\omega_0}{N_{eff}} f_{rep} \tag{2}$$

Under this consideration, different scans will be carried out by varying the speed and the overlap separation (Δy), which corresponds to the distance between each scan, as shown in Figure 3. To establish the separation Δy, the criterion is based on the measurement of the diameter of the area defined by the LIPSS in the punctual irradiations.

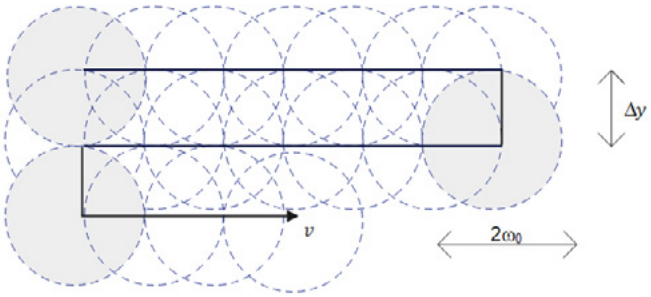

Figure 3.

Representative scheme of scans generated by superimposed laser pulses. The separation between each scan is Δy, the diameter of the incident beam is defined by $2\omega_0$, v indicates the direction of the scanning speed.

3. Results and discussion

To determine the threshold combination of laser pulse fluence and number of pulses that produce LIPSS, a matrix like the one shown in Figure 4, exploring

several combinations of these parameters was constructed. This method allows for a controlled investigation of the impact of the laser on the material, ensuring that the influence of each pulse is carefully examined. It is important to note that each column of the matrix corresponds to a different fluence, having a 5% variation, while each row represents a different number of pulses. It was found that at a per pulse fluence of 16.2 J/cm^2 and a range of pulses between 1 and 30, images with the physical appearance of LIPSS were obtained. Figure 4 shows only the lowest laser fluence values for which changes in the samples were detected. This systematic and controlled approach contributes to a more nuanced understanding of the laser-material interaction, paving the way for targeted applications in surface engineering and microfabrication.

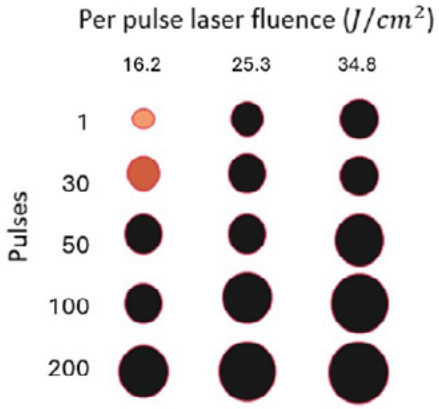

Figure 4.

Matrix of irradiation using Al thin films.

Using equation 2, it was possible to determine the speed at which the sample should be transported (8 $\mu m/s$), resulting in 4 effective pulses with a frequency of 1 Hz. Following the methodology described in the previous section, a Δy = 60 μm distance was determined. According to the methodology followed, such distance is greater than the corresponding one, but when the experiment was carried out with smaller distances, the film completely detached from the substrate.

Figure 5 shows the micrographs of the samples in Al thin films obtained with an optical microscope, specifically an Olympus (BX41), known for its precision and ability to accurately measure the characteristics of complex surfaces such as LIPSS. These samples were also examined using a profilometer, resulting in a maximum depth of 300 nm.

By analyzing these micrographs, it was determined that the structures do not correspond to LIPSS, although they presented some similar physical characteristics to those of the LIPSS. This discrepancy can be attributed to several

factors. First, LIPSS are characterized by their precise periodicity and alignment relative to the laser polarization, and the observed structures lack this specific periodicity or orientation, indicating a different formation mechanism. Upon visual inspection, the samples might display patterns that superficially resemble the typical features of LIPSS, such as line-like formations and regular arrays, but detailed imaging reveals an absence of any consistent periodicity. Second, although the samples may display patterns resembling LIPSS, their microstructural features (such as depth, spacing, and uniformity) differ due to variations in laser parameters or material properties during processing. This further underscores the processes' complexity and suggests that the observed phenomena might stem from different interactions between the laser and the material surface.

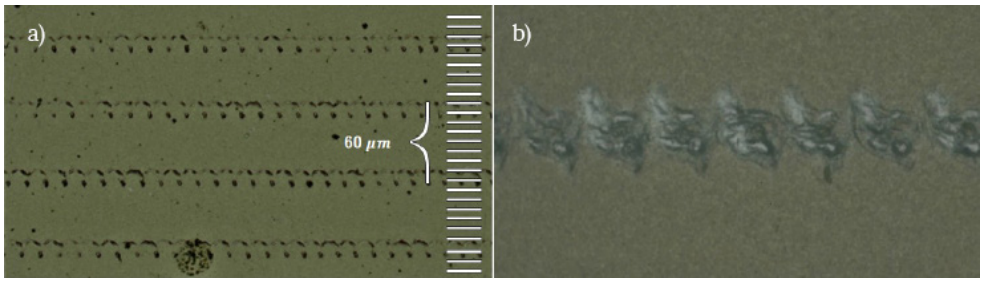

Figure 5.

Observed micrographs of the samples in Al thin films, *a*) With 20X objective, *b*) With 40X objective.

4. Conclusion

The experimental results decisively demonstrate that generating LIPSS on Al thin films under the utilized conditions is impractical. This finding aligns with the study by Reyes-Contreras *et al.* [2], which also highlighted the limitations in laser parameters and material properties for forming LIPSS on thin metal films.

The research establishes that achieving overlap in Al thin films is unattainable within the experimental parameters. In previous studies, such as that by Santillan *et al.* [3], it has been indicated that the overlap of LIPSS can be influenced by the laser fluence and film thickness, suggesting the need to adjust these parameters to obtain optimal results carefully.

The observed structures differ from LIPSS in terms of periodicity, orientation, and microstructural features. These differences arise from variations in laser parameters and material properties during processing, corroborating observations from other studies, such as those by Robles *et al.* [5] and Segovia *et al.* [6]. Further research to optimize laser parameters and explore alternative materials could provide insights into overcoming these limitations.

Additional studies, such as those by Chang *et al.* [7] and González-Parra *et al.* [8], suggest that exploring new laser techniques and materials could enhance our understanding of LIPSS formation and improve the reproducibility of these structures.

5. Funding

The authors acknowledge funding from Mexico's National Council of Humanities, Science, and Technology (Conahcyt) through grant No. CF-2019-102986).

6. Acknowledgments

The authors acknowledge funding from Mexico's National Council of Humanities, Science, and Technology (Conahcyt) through grant No. CF-2019-102986).

References

[1] A. Wong Gutiérrez, "Optimización del proceso de generación de LIPSS en metales con pulsos ultra-cortos," Centro de Investigación Científica y de Educación Superior de Ensenada, Baja California, Ensenada, Baja California, México, 2019, https://repositorionacionalcti.mx/recurso/oai:cicese.repositorioinstitucional.mx:1007/2761

[2] A. Reyes-Contreras, M. Camacho-López, S. Camacho-López *et al.*, "Laser-induced periodic surface structures on bismuth thin films with ns laser pulses below ablation threshold," *Optical Materials Express* **7**(6), 1777 (2017), https://doi.org/10.1364/OME.7.001777

[3] R. Santillan, A. Wong, P. Segovia *et al.*, "Femtosecond laser-induced periodic surface structures formation on bismuth thin films upon irradiation in ambient air," *Optical Materials Express* **10**(2), 674 (2019), https://doi.orvvg/10.1364/OME.384019

[4] S. Camacho-López, R. Evans, L. Escobar-Alarcón *et al.*, "Polarization-dependent single-beam laser-induced grating-like effects on titanium films," *Applied Surface Science* **255**(5), 3028–3032 (2008), https://doi.org/10.1016/j.apsusc.2008.08.085

[5] V. Robles, J. C. Gonzalez-Parra, N. Cuando-Espitia *et al.*, "The effect of scalable PDMS gas-entrapping microstructures on the dynamics of a single cavitation bubble," *Scientific Reports* **12**(1), (2022), https://doi.org/10.1038/s41598-022-24746-w

[6] P. Segovia, A. Wong, R. Santillan *et al.*, "Multi-phase titanium oxide LIPSS formation under fs laser irradiation on titanium thin films in ambient air," *Optical Materials Express* **11**(9), 2892 (2021), https://doi.org/10.1364/OME.431210

[7] J. T. Chang, C. H. Yeh, J. L. He *et al.*, "Cavitation erosion and corrosion behavior of Ni–Al intermetallic coatings," *Wear* **255**(1–6), 162–169 (2003), https://doi.org/10.1016/S0043-1648(03)00199-6

[8] J. C. Gonzalez-Parra, V. Robles, L. F. Devia-Cruz *et al.*, "Mitigation of cavitation erosion using laser-induced periodic surface structures," *Surfaces and Interfaces* **29**, 101692, (2021), https://doi.org/10.1016/j.surfin.2021.101692

[9] A. Fraijo Rodas, "Efecto de la polarización en la formación de LIPSS en bismuto," Centro de Investigación Científica y de Educación Superior de Ensenada, Baja California, Ensenada, Baja California, México, 2021, https://cicese.repositorioinstitucional.mx/jspui/bitstream/1007/3575/1/tesis_Abigail%20Fraijo%20Rodas_03%20junio%202021.pdf